Proceedings of the International Conference on LASERS'88
Lake Tahoe, Nevada, Dec. 4-9, 1988
R.C. Sze and F.J. Duarte, Editors, STS Press, McLean, VA, 1989

INTENSE ULTRASHORT PULSE GENERATION IN TWO-PHOTON PUMPED DYE LASER GENERATORS AND AMPLIFIERS

A. Penzkofer and P. Qiu *
Naturwissenschaftliche Fakultät II - Physik,
Universität Regensburg, D-8400 Regensburg, Fed.Rep.Germany

* Shanghai Institute of Optics and Fine Mechanics,
Academia Sinica, Shanghai, P.R. China

The dyes rhodamine B, rhodamine 6G and PYC are excited by two-photon absorption of light pulses of a passively mode-locked Nd-glass laser. Ultrashort light pulses in the spectral range between 565 and 630 nm are generated by two-photon induced amplified spontaneous emission (TPI-ASE) and two-photon induced seeding pulse amplification (TPI-SPA) of picosecond light continua. The generated signals are amplified in a two-photon pumped dye laser amplifier (TPI-AMP).

1. Introduction

The single-photon pumped amplified spontaneous emission (SPI-ASE) in organic dyes allows the generation of frequency tunable ultrashort light pulses at the Stokes-side of fixed-frequency pump lasers. Longitudinal[1,2], transversal[3], and travelling-wave transverse[4-6] pumping techniques are applied. The selective spectral amplification of ultrashort light continua in single-photon pumped organic dye solutions (single-photon induced seeding pulse amplification SPI-SPA) is applied in frequency tunable picosecond[1,2] and femtosecond pulse generation[7,8].

The two-photon pumped amplified spontaneous emission (TPI-ASE)[9-11] and the two-photon pumped seeding pulse amplification (TPI-SPA)[11] of ultrashort light continua in organic dye solutions allow the generation of frequency tunable ultrashort light pulses in the wavelength region between the fundamental and second harmonic frequency. The generated signals may be amplified in two-photon pumped dye laser amplifiers (TPI-AMP)[11].

In this paper first the two-photon pumped amplified spontaneous emission and seeding pulse amplification are compared with single photon pumping. In the experiments a passively mode-locked Nd-glass laser[12] serves as pump source for the pulse generation by TPI-ASE, TPI-SPA, and TPI-AMP. The dyes rhodamine B in hexafluoroisopropanol and methanol, rhodamine 6G in HFIP, and PYC (1,3,1',3 -tetramethyl-2,2'-dioxopyrimido-6,6'-carbocyanine hydrogen sulfate)[13] in HFIP have been investigated. Frequency tunable light pulses in the wavelength region between 565 nm and 630 nm have been generated. Energy conversion efficiencies up to 3.5 percent have been obtained in a two-photon pumped generator-amplifier system. The divergence of the generated light is as small as $\Delta\theta \approx 7\times10^{-4}$ rad.

2. Fundamentals

The dynamics of single-photon induced and two-photon induced ASE, SPA, and AMP are illustrated in the dye configuration coordinate diagrams of Fig.1a and 1b, respectively. The schematic experimental arrangements of amplified spontaneous emission (dye laser generator), seeding pulse amplification, and signal amplification (dye laser amplifier) are depicted in Figs.2a-2c.

The single-photon pumped ASE, SPA, and AMP are described roughly by the equations 1-3. A more detailed equation system is given in Ref.1.

$$\frac{\partial N_{S1}}{\partial t} \approx \frac{1}{h\nu_L}\,\sigma_L(N_0-N_{S1})I_L \tag{1}$$

$$\frac{\partial I_L}{\partial z} \approx -\sigma_L(N_0-N_{S1})I_L - \sigma_{ex}^{L}N_{S1}I_L \tag{2}$$

$$\frac{\partial I_F}{\partial z} \approx h\nu_F \frac{N_{S1}}{\tau_{rad}}\frac{\Delta\Omega}{4\pi} + (\sigma_F - \sigma_F^{ex})N_{S1}I_F \tag{3}$$

N_{S1} is the number density of dye molecules in the S_1-state. N_0 is the total number density of dye molecules. Eq.1 describes the S_1-state population. The absorption of the pump pulse is given by Eq.2. The first term is due to ground-state absorption and the second term is due

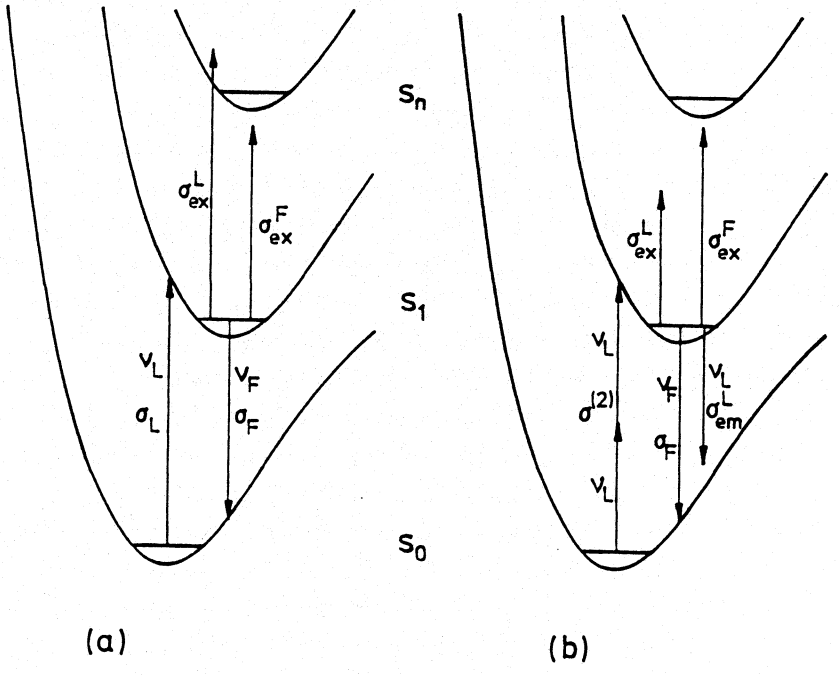

Fig.1: Single-photon induced (a) and two-photon induced (b) dynamics in configuration coordinate systems of dyes.

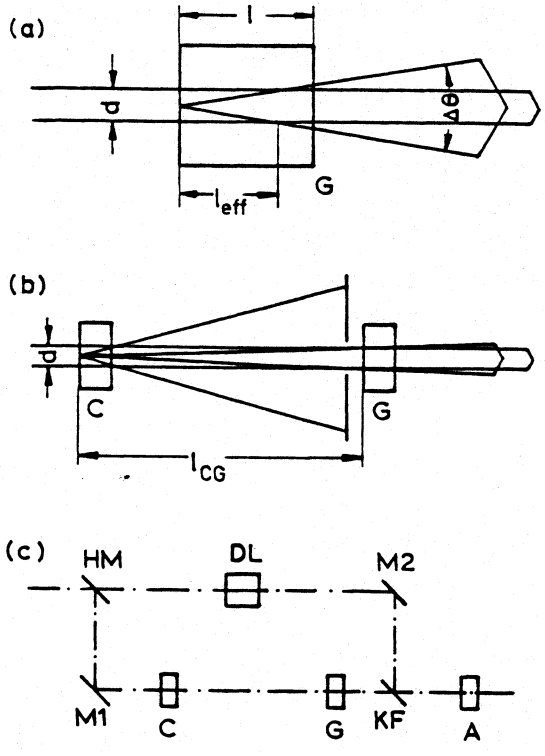

Fig.2: Schematic experimental layouts for (a) two-photon pumped amplified spontaneous emission (TPI-ASE) in generator cell G, (b) two-photon pumped seeding pulse amplification (TPI-ASE), and (c) two-photon pumped generator-amplifier system. C, cell for generation of ps light continuum. G, dye generator cell. A, dye amplifier cell. HM, 50 %-mirror, M1, and M2, 100 %-mirrors. KF, short-pass edge filter. DL, delay block.

to excited state absorption. Eq.3 handles the light emission. The first term gives the spontaneous emission. τ_{rad} is the radiative lifetime of the S_1-state and $\Delta\theta$ is the solid angle of efficient amplified spontaneous emission [$\Delta\Omega = \pi(\Delta\theta)^2/4$, $\Delta\theta$ beam divergence of generated light]. The second term of Eq.3 is due to stimulated emission and describes the amplification of spontaneous emission (no input signal), the seeding pulse amplification (input of light continuum), and the signal amplification (input of ASE or SPA-signal).

Solution of Eq.3 gives an amplification factor (gain) $G = I_{F,out}/I_{F,in}$ of

$$G \approx \exp[(\sigma_F - \sigma_F^{ex}) N_{S1} \ell_{eff}] \tag{4}$$

The dye concentrations in single-photon pumping are low and the pump pulses bleach the ground-state absorption at the cell entrance. The pump pulse penetration length ℓ_{eff} is derived from the relation (solution of Eq.2) $T \approx \exp\{-[\sigma_L(N_0 - N_{S1}) + \sigma_{ex}^L N_{S1}]\ell_{eff}\} \lesssim \exp\{-\sigma_{ex}^L N_0 \ell_{eff}\} = \exp(-1)$ to be

$$\ell_{eff} \lesssim (N_0 \sigma_{ex}^L)^{-1} \tag{5}$$

The amplification factor is limited to (insertion of Eq.5 into Eq.4 with $N_{S1} \to N_0$)

$$G \lesssim \exp\left(\frac{\sigma_F - \sigma_{ex}^F}{\sigma_{ex}^L}\right) \tag{6}$$

For optimum signal output the dye cell length ℓ should be approximately equal to ℓ_{eff} in order to avoid reabsorption of generated light at frequency ν_F due to reabsorption in unexcited dye regions.

The two-photon pumped ASE, SPA, and AMP are described roughly by the Eqs.7-9. A detailed description is given in Ref.10.

$$\frac{\partial N_{S1}}{\partial t} \approx \frac{1}{2(h\nu_L)^2} \sigma^{(2)} N_0 I_L^2 - \frac{1}{h\nu_L} \sigma_{em}^L N_{S1} I_L \tag{7}$$

$$\frac{\partial I_L}{\partial z} \approx -\frac{1}{h\nu_L} \sigma^{(2)} N_0 I_L^2 + \sigma_{em}^L N_{S1} I_L - \sigma_{ex}^L N_{S1} I_L \tag{8}$$

$$\frac{\partial I_F}{\partial z} \approx h\nu_F \frac{N_{S1}}{\tau_{rad}} \frac{\Delta\Omega}{4\pi} + (\sigma_F - \sigma_F^{ex}) N_{S1} I_F \tag{9}$$

The first term of Eq.7 gives the S_1-state population by two-photon absorption. The second term is responsible for the S_1-level depopulation by stimulated emission. This term reduces the light amplification factor G at frequency ν_F since it reduces the S_1-level population. The stimulated emission at frequency ν_L does add to the pump pulse intensity (second term of Eq.8) but two pump pulse photons are absorbed (first term of Eq.7) and only one photon is returned. The equation of amplified spontaneous emission and stimulated emission (Eq.9) is identical to Eq.3. The amplification factor G is again given by Eq.4. High dye concentrations are needed in two-photon pumping to absorb the pump pulse effectively at reasonable pump pulse intensities (avoidance of dielectric breakdown or other nonlinear optical processes like stimulated Raman scattering) and sample lengths (order of confocal length of lenses). The pump pulse generally does not deplete remarkably the ground-state population and the S_1-state population at the cell entrance is approximately

$$N_{S1} \approx \frac{1}{2(h\nu_L)^2} \sigma^{(2)} N_0 I_L^2 \Delta t_L \tag{10}$$

The effect of stimulated emission at the pump pulse frequency is neglected. Δt_L is the pump pulse duration. In most cases the excited state absorption of the pump laser determines the effective interaction length ℓ_{eff}. The two-photon transmission is $T \approx \exp(-\sigma_{ex}^L N_{S1} \ell_{eff}) / \{1+\sigma^{(2)} N_{S1} I_L [1-\exp(-\sigma_{ex}^L N_{S1} \ell_{eff})]/(\sigma_{ex}^L N_{S1})\} < \exp(-\sigma_{ex}^L N_{S1} \ell_{eff})$ and the condition $T = \exp(-1)$ gives

$$\ell_{eff} < (\sigma_{ex}^L N_{S1})^{-1} \approx \frac{2(h\nu_L)^2}{\sigma_{ex}^L \sigma^{(2)} N_0 I_L^2 \Delta t_L} \tag{11}$$

The maximum possible amplification factor is again given by Eq.6. The sample length should be approximately equal to ℓ_{eff}.

In the case of two-photon pumping, σ_{ex}^L may be smaller than in the case of single photon pumping (Fig.1) so that higher amplification factors may be obtainable. For the same dyes single photon pumping would require pumping with the second harmonic light of the pump laser which reduces the over-all efficiency.

For amplified spontaneous emission the generated pulse durations Δt_F ($\Delta t_F < \ln(2)\tau_F$, τ_F is lifetime of spontaneous emission) depend strongly on the amplification factor G (and bottle-neck effects[1,10,11]). The seeding pulse amplification of pump-pulse generated light continua gives pulse durations of approximately $\Delta t_F \approx \Delta t_L/3$.

3. Results

3.1 Dyes. Spectroscopic parameters of the investigated dyes are listed in Table 1. Further informations are given in Ref.11. The absorption cross-section spectrum and stimulated emission cross-section spectrum[16] of rhodamine B in HFIP is depicted in Fig.3. The wavelength positions of two-photon excitation $\lambda_L/2$, excited state absorption λ_{ex}^L and λ_{ex}^F together with the region λ_F of amplified spontaneous emission (FWHM) are included.

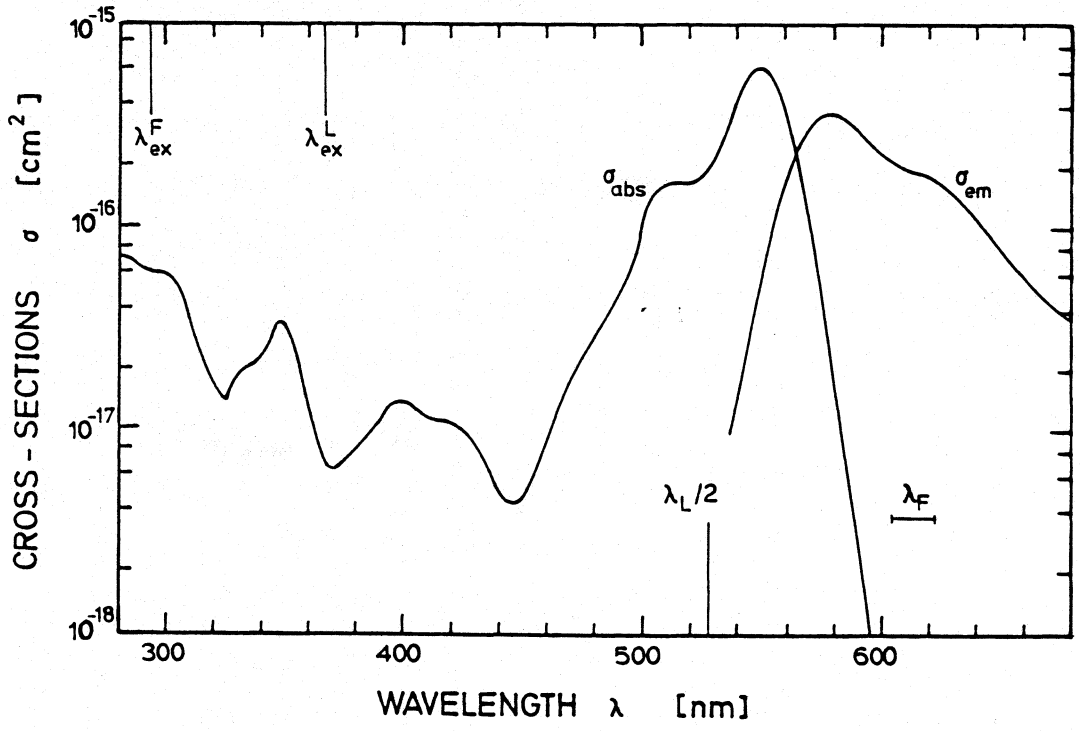

Fig.3: Absorption and emission cross-section spectrum of rhodamine B in hexafluoroisopropanol (HFIP).

3.2 Two-photon absorption. The measured energy transmissions of picosecond pump pulses ($\Delta t_L \approx 5$ ps, $\lambda_L = 1.055$ µm) through 10^{-2} molar rhodamine B in HFIP are shown by the open circles of Fig.4. The solid curve is calculated by fitting the two-photon absorption cross-section $\sigma^{(2)}$ and the excited-state absorption cross-section σ_{ex}^L [10] (see Table 1). The solid circles and the dashed curve belong to the solvent HFIP. Above 1.5×10^{11} W/cm² the pump pulse transmission through the solvent reduces drastically by nonlinear optical effects. The solid energy transmission curve indicates optimum intensity conditions for amplified spontaneous emission around $I_{0L} \approx 1.5\times10^{11}$ W/cm². The two-photon absorption parameters $\sigma^{(2)}$ and σ_{ex}^L of the investigated dyes are listed in Table 1.

3.3 Two-photon induced seeding pulse amplification (TPI-ASE). The displayed results belong to 0.01 molar rhodamine B in HFIP. In Table 1 results are summarized for the other dye solutions.

Fig.5a displays the ASE-energy conversion efficiency η_E versus pump pulse input intensity I_{0L}. The sample length is $\ell = 2$ cm. The circles are measured and the curve is calculated.[10,11] The energy conversion efficiency rises steeply and saturates above $I_{0L} \approx 10^{11}$ W/cm² (see Eq.6). The energy conversion efficiency versus sample length is depicted in Fig.5b for $I_{0L} = 1.5\times10^{11}$ W/cm². Gain saturation is observed for sample lengths $\ell > 1$ cm.

The wavelength of maximum ASE emission, $\lambda_{F,max}$, (dash-dotted curve) and the spectral half-width of the ASE emission (width of hatched region) are shown versus pump pulse peak inten-

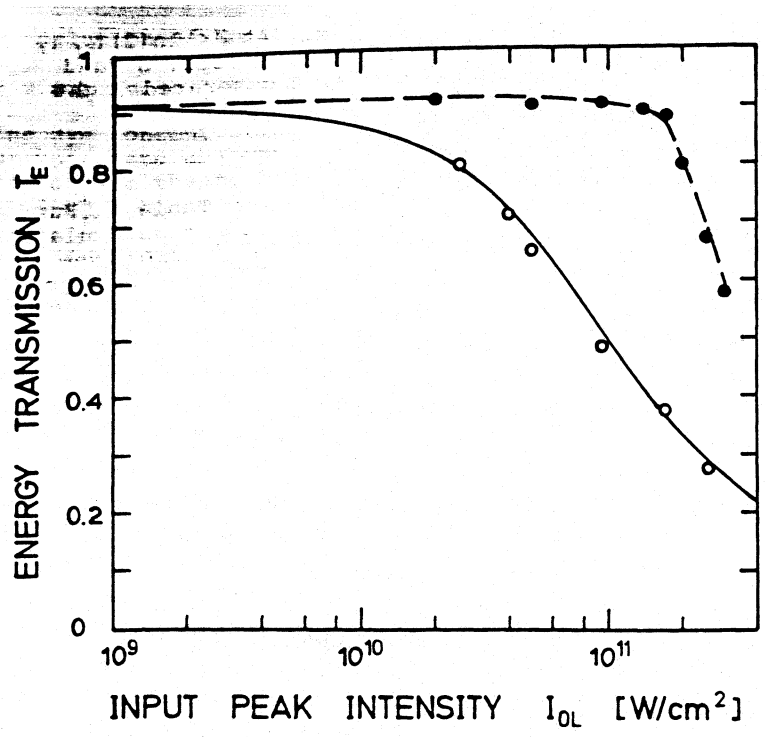

Fig.4: Energy transmission of pump pulses (λ_L = 1.055 µm, Δt_L = 5 ps) through 0.01 molar rhodamine B in HFIP (solid curve) and pure solvent HFIP (dashed curve). Sample length ℓ = 2 cm.

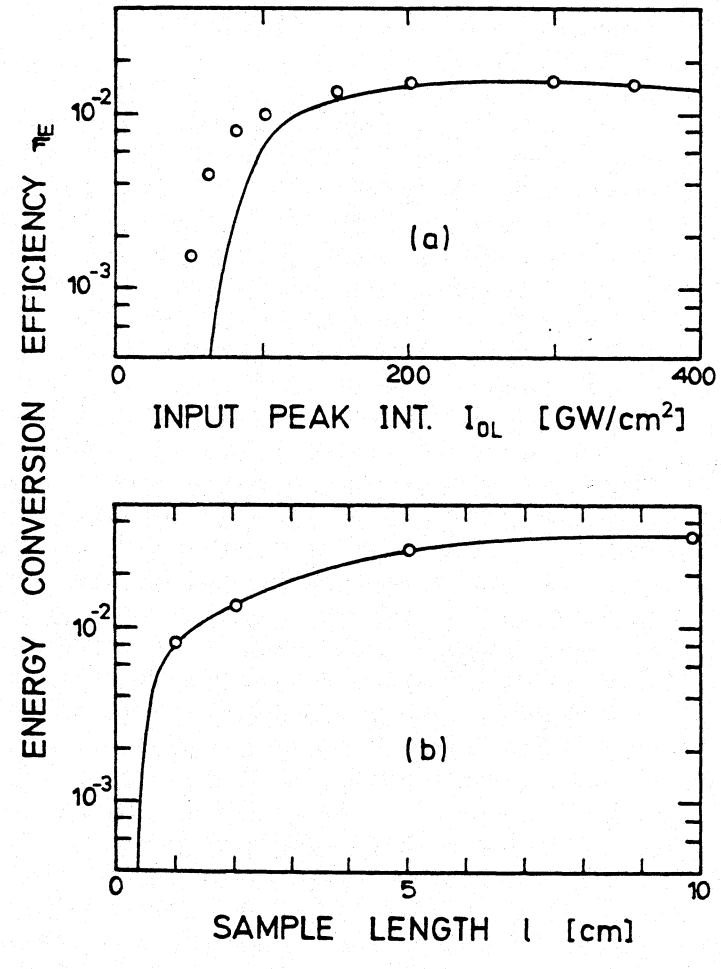

Fig.5: Energy conversion efficiency η_E of TPI-ASE versus (a) pump pulse peak intensity I_{0L} (ℓ = 2 cm, solid curve calculated[11]) and (b) sample length ℓ (I_{0L} = 1.5×10^{11} W/cm^2). Dye: 0.01 molar rhodamine B in HFIP.

sity in Fig.6a. The sample length is ℓ = 2 cm. $\lambda_{F,max}$ versus sample length is displayed in Fig.6b for $I_{0L} = 1.5\times10^{11}$ W/cm². The wavelength of maximum emission shifts to longer wavelengths with sample length because of fluorescence light reabsorption (see long-wavelength absorption tail of Fig.3). The spectral distribution of an ASE signal (ℓ = 2 cm, $I_{0L} \approx 1.5\times10^{11}$ W/cm²) is reproduced in Fig.7a. The spectral distribution is rather flat (averaging over ASE-divergence angle).

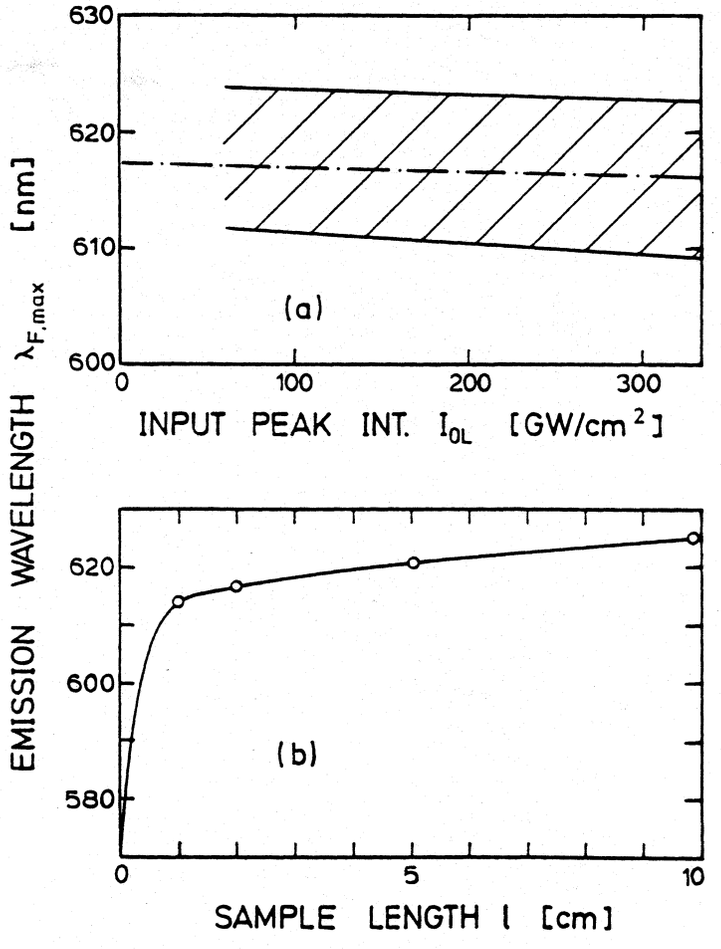

Fig.6: Wavelength of peak TPI-ASE emission versus (a) pump pulse peak intensity I_{0L} (ℓ = 2 cm) and (b) sample length ℓ ($I_{0L} = 1.5\times10^{11}$ W/cm²). Hatched region of (a) indicates spectral width (FWHM). Dye is 0.01 molar rhodamine B in HFIP.

The dependence of the ASE divergence $\Delta\Theta$ on the input pump pulse peak intensity for ℓ = 2 cm and on the sample length for $I_{0L} = 1.5\times10^{11}$ W/cm² are depicted in Figs.8a and b, respectively. At low intensities the divergence increases drastically because of reduced gain, and at high intensities the divergence increases because of shorter effective interaction length ℓ_{eff} (Eq.11, $\Delta\Theta \approx d/\ell_{eff}$, d beam diameter of pump pulse, see Fig.2a).

Calculated results of the ASE-pulse duration versus pump pulse peak intensity (ℓ = 2 cm) are presented in Fig.9[11]. The ASE pulse duration shortens strongly with increasing pump pulse intensity. Above $I_{0L} \approx 8\times10^{10}$ W/cm² the ASE pulse duration Δt_F becomes shorter than the pump pulse duration Δt_L (dashed-dotted line). The inset of Fig.9 shows the temporal shape of the pump pulse (dashed curve) and of the ASE pulse at $I_{0L} = 1.5\times10^{11}$ W/cm² (solid curve).

3.4 Two-photon induced seeding pulse amplification (TPI-SPA). For the seeding pulse amplification experiments, the picosecond light continuum is generated in a 2 cm long D_2O cell[15] (Fig.2b). At $I_{0L} \approx 1.5\times10^{11}$ W/cm² the energy conversion efficiency of the light continuum within a spectral width of $\Delta\lambda$ = 10 nm around 600 nm is approximately 5×10^{-5}. The seeding pulse amplification reduces drastically the divergence of the spectrally selective amplified light continuum ($\Delta\Theta \approx d/\ell_{CG}$, ℓ_{CG} distance between D_2O cell and dye cell, see Fig.2b). A spectral distribution of the SPA signal generated by 0.01 molar rhodamine B in HFIP (ℓ = 2 cm, $I_{0L} \approx 1.5\times10^{11}$ W/cm²) is displayed in Fig.7b. The spectrum is strongly structured because the divergence angle $\Delta\Theta$ becomes comparable to the coherence angle of the generated light[1,17]. The energy conversion efficiency of the SPA light is approximately the same as in the case of the ASE light, but the divergence is drastically reduced. Results of the energy conversion efficiency and of the beam divergence are listed in Table 1. The wavelengths of maximum spectral emission $\lambda_{F,max}$ and the spectral widths (FWHM) of emission are approximately

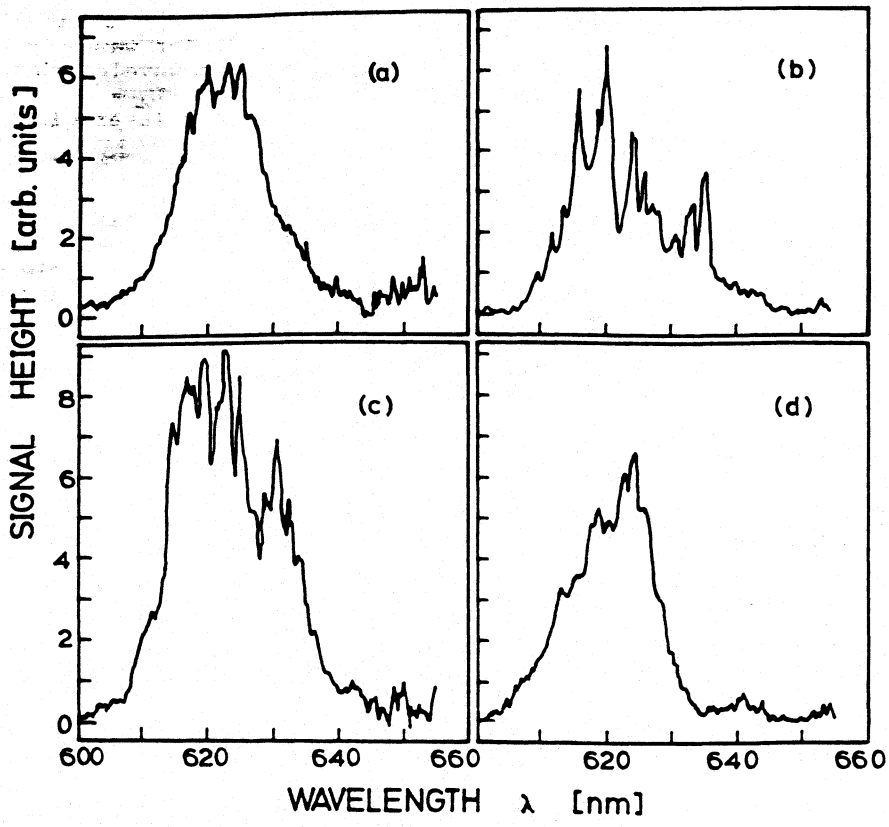

Fig.7: Spectral distributions of 0.01 molar rhodamine B in HFIP. Cell lengths ℓ = 2 cm. Pump pulse peak intensities $I_{0L} \approx 1.5\times10^{11}$ W/cm². (a) TPI-ASE. (b) TPI-SPA. (c) amplified ASE signal. (d) amplified SPA-signal.

the same as in the case of amplified spontaneous emission.

3.5 Two-photon induced signal amplification (TPI-AMP). The TPI-ASE and the TPI-SPA signals may be further increased in energy, and the divergence may be further reduced in two-photon pumped dye laser amplifiers. Behind the dye generator cell spectral narrowing and spectral tuning is possible to generate narrow-band spectrally tunable light pulses.

With the experimental arrangement of Fig.2c, TPI-ASE and TPI-SPA signals have been amplified. In the generator cell and in the amplifier cell 0.01 molar rhodamine B in HFIP was applied in 2 cm long cells. The over-all energy conversion efficiency (signal behind amplifier to total input signal before beam splitter, Fig.2c) was a few percent (for TPI-ASE: $\eta_E \approx 0.02$; for TPI-SPA: $\eta_E \approx 0.035$). The beam divergence of the generated light behind the amplifier was $\Delta\theta \approx 7\times10^{-4}$ rad. Spectral distributions are shown in Fig.7c and d.

4. Conclusions

The two-photon pumped amplified spontaneous emission, seeding pulse amplification, and signal amplification allows to generate frequency tunable ultrashort light pulses at the anti-Stokes side of ultrashort fixed-frequency pump lasers. The over-all efficiency of two-photon pumped amplified spontaneous emission is very likely higher than the single-photon pumped amplified spontaneous emission which employs the second harmonic of the pump pulses. Very often the excited-state absorption of the second harmonic light is higher than the excited state-absorption of the fundamental light, which favours the two-photon pumped amplified spontaneous emission.

For the TPI-ASE and TPI-SPA experiments laser dyes and fast saturable absorbers may be employed. In TPI-ASE experiments the generated pulse duration is strongly gain dependent and fast picosecond saturable absorbers give shorter pulse durations than laser dyes with nanosecond fluorescence lifetime. The seeding pulse amplification of pump-pulse generated parametric light continua generates pulse durations of typically one third of the pump pulse duration.

Two-photon pumped generator-amplifier systems may be applied to other picosecond and femtosecond pump sources. They may be very fruitful for the generation of frequency tunable ultrashort light pulses in the near ultraviolet spectral region by employing visible pump pulses. Besides dyes other laser materials may be employed in two-photon pumped generator-amplifier systems (e.g. semiconductors[18]).

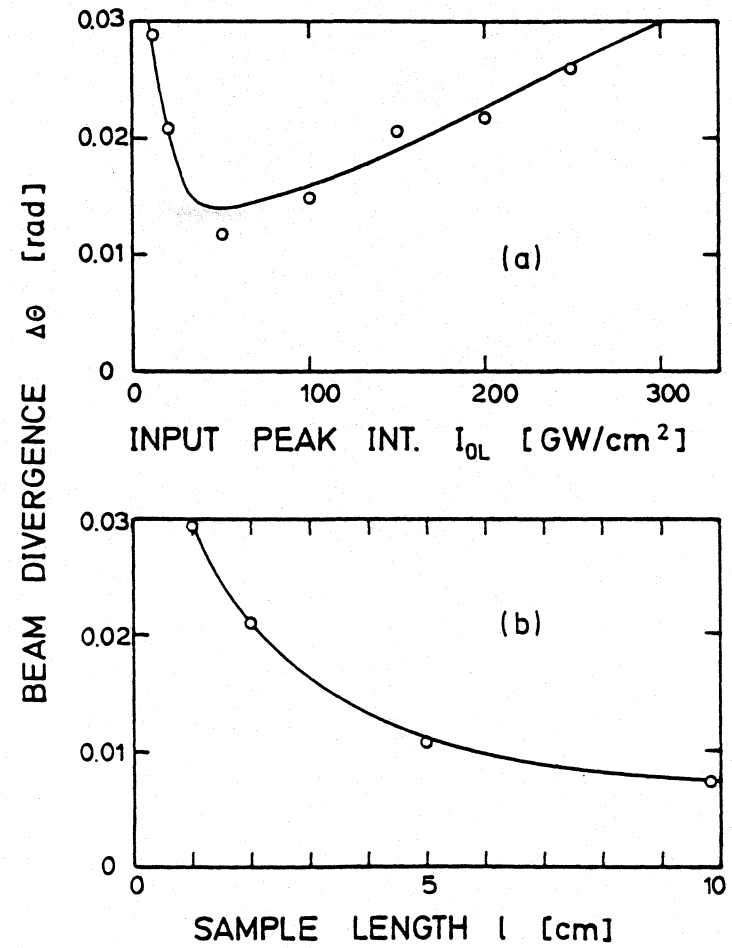

Fig.8: Beam divergence $\Delta\theta$ of TPI-ASE signal versus (a) pump pulse peak intensity I_{0L} (ℓ = 2 cm) and (b) sample length ℓ ($I_{0L} \approx 1.5\times10^{11}$ W/cm²). Dye: 0.01 molar rhodamine B in HFIP.

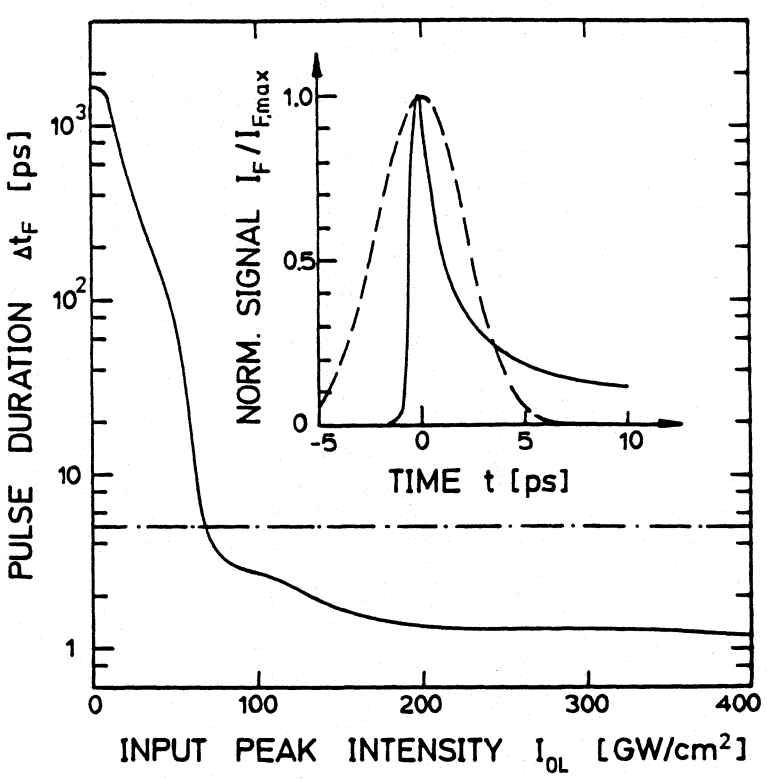

Fig.9: Calculated duration of TPI-ASE signal versus pump pulse peak intensity I_{0L} (sample length ℓ = 2 cm, dye concentration 0.01 mol/dm³). Dye parameters of rhodamine B in HFIP (Table 1) are used. Dashed-dotted line indicates pump pulse duration Δt_L. Inset gives temporal pulse shape of pump pulse (dashed curve) and of ASE-signal at $I_{0L} = 1.5\times10^{11}$ W/cm².

Table 1: Dye parameters and dye performance data. ASE and SPA data belong to dye concentrations of $C = 10^{-2}$ mol/dm³ and pump pulses of $\lambda_L = 1.055$ μm, $\Delta t_L = 5$ ps, and $I_{0L} = 1.5\times10^{11}$ W/cm².

Parameter	Rhodamine B		Rhodamine 6G	PYC
Solvent	HFIP	Methanol	HFIP	HFIP
$\sigma^{(2)}$ [cm⁴s]	1.5×10^{-49}	1.5×10^{-49}	1×10^{-49}	1.8×10^{-49}
σ_{ex}^{L} [cm²]	1×10^{-17}	1.5×10^{-17}	5×10^{-18}	$\lesssim 2\times10^{-18}$
$\lambda_{F,max}$ [nm]	617	620	570	600
σ_F [cm²]	1.9×10^{-16}	1.5×10^{-16}	1.5×10^{-16}	1.85×10^{-16}
σ_{ex}^{F} [cm²]	3×10^{-17}	1×10^{-17}	9×10^{-17}	7.5×10^{-17}
τ_F [ns]	2.4	1.17	4.1	0.011
TPI-ASE				
η_E	1.3×10^{-2}	7×10^{-3}	5×10^{-4}	7×10^{-3}
$\Delta\theta$ [rad]	2×10^{-2}	2×10^{-2}	2.5×10^{-2}	2×10^{-2}
$\Delta\lambda_F$ [nm]	13	20	8.5	12
Δt_F [ps]	1.7	4.5	10	0.35
TPI-SPA				
η_E	1×10^{-2}	7×10^{-3}	1×10^{-3}	3×10^{-3}
$\Delta\theta$ [rad]	1.8×10^{-3}	2.5×10^{-3}	2×10^{-3}	3×10^{-3}

References

1. P. Sperber, W. Spangler, B. Meier, and A. Penzkofer, Opt. Quantum Electron. 20, 395 (1988).
2. P. Sperber, W. Spangler, B. Meier, and A. Penzkofer, in Proceedings, International Conference on Lasers'87, D.A. Duarte, Ed. (STS Press, McLean, VA, 1988) pp. 370-377.
3. C. Lin, T.K. Gustafson, and A. Dienes, Opt. Commun. 8, 210 (1973).
4. Zs. Bor and A. Müller, IEEE J. QE-22, 1524 (1986).
5. T. Elsaesser, H.J. Polland, A. Seilmeier, and W. Kaiser, IEEE J. QE-20, 191 (1984).
6. W. Lee, C. Ning, and Z. Huang, Appl. Phys. B40, 35 (1986).
7. A. Migus, I.L. Martin, R. Astier, A. Antonetti, and A. Orizag, in Picosecond Phenomena III, K.B. Eisenthal, R.M. Hochstrasser, W. Kaiser, and A. Laubereau, Eds. (Springer-Verlag, Heidelberg, 1982) pp.6-9.
8. P.C. Becker, H.L. Fragnito, R.L. Fork, F.A. Beisser, and C.V. Shank, in Ultrafast Phenomena VI, T. Yajima, K. Yoshihara, C.B. Harris, and S. Shionoya, Eds. (Springer-Verlag, Heidelberg, 1988) pp. 12-14.
9. V.I. Prokohorenko and E.A. Tikhonov, Sov. J. Quant. Electron. 16, 1214 (1986).
10. A. Penzkofer and W. Leupacher, Opt. Quantum Electron. 19, 327 (1987).
11. P. Qiu and A. Penzkofer, Appl. Phys. B, to be published.
12. A. Penzkofer and F. Graf, Opt. Quantum Electron. 17, 219 (1985).
13. A. Penzkofer, W. Leupacher, B. Meier, B. Runde, and K.H. Drexhage, Chem. Phys. 115, 143 (1987).
14. A. Penzkofer and W. Kaiser, Appl. Phys. Letters 21, 427 (1972).
15. A. Penzkofer and W. Kaiser, Opt. Quantum Electron. 9, 315 (1977).
16. A. Penzkofer and W. Leupacher, J. Luminesc. 37, 61 (1987).
17. L. Mandel and E. Wolf, Rev. Mod. Phys. 37, 231 (1965).
18. A. Penzkofer and A.A. Bugayev, Opt. Quantum Electron., to be published.